Limits for Reduction of Acquisition Time and Administered Activity in ^{18}F-FDG PET Studies of Alzheimer Dementia and Frontotemporal Dementia

Florian Schiller[1], Lars Frings[1,2], Johannes Thurow[1], Philipp T. Meyer[1], and Michael Mix[1]

[1]*Department of Nuclear Medicine, Medical Center–University of Freiburg, Freiburg, Germany; and* [2]*Center for Geriatrics and Gerontology, Medical Center–University of Freiburg, Freiburg, Germany*

We evaluated the effect of a reduced acquisition time for ^{18}F-FDG PET studies of Alzheimer dementia (AD) and frontotemporal dementia (FTD) to derive a limit for reductions of acquisition time (improving patient compliance) and administered activity (lowering the radiation dose) with uncompromised diagnostic outcome. **Methods:** We included patients with a clinical diagnosis of AD (n = 13) or FTD (n = 12) who were examined with ^{18}F-FDG PET/CT after injection of 210 ± 9 MBq of ^{18}F-FDG. List-mode data were reconstructed over various time intervals simulating reduced acquisition times or administered activities. Volume-of-interest–based and voxelwise statistical analyses including group contrasts were performed for 15 different acquisition times ranging from 10 min to 2 s. In addition, masked visual reads were obtained from 3 readers independently for 7 different acquisition times down to 30 s, providing a diagnosis of either AD or FTD and the individual diagnostic certainty. **Results:** Regional mean uptake changed by less than 5% at a reduced acquisition time down to 1 min in all regions and patients except for the posterior cingulate cortex of 1 patient. Voxelwise group contrasts suggest a sufficient measurement time of only 2 min, for which the number of significant voxels decreased by merely 5% while maintaining their spatial pattern. In 450 visual reads at reduced times, no change in the original diagnosis was observed. The diagnostic certainty showed only a very slow and mild decline, with small effect sizes (Cohen's d) of 0.3, at acquisition times of 3 and 2 min compared with the original results at 10 min. **Conclusion:** Statistical results at a region and voxel level, as well as single-subject visual reads, reveal a considerable potential to reduce the typical 10-min acquisition time (by a factor of 4) without compromising diagnostic quality. Conversely, our data suggest that for a given acquisition time of 10 min and a similar effect size, the administered activity may be reduced to 50 MBq, resulting in an effective dose of less than 1 mSv for the PET examination.

Key Words: brain ^{18}F-FDG PET/CT; acquisition time; dose; dementia; neurodegenerative disorders

J Nucl Med 2019; 60:1764–1770
DOI: 10.2967/jnumed.119.227132

For detecting neuronal degeneration in neurodegenerative disorders such as dementia, parkinsonism, and their prodromal stages, ^{18}F-FDG PET is a valuable and well-established diagnostic method (*1–3*). Disease-specific metabolism patterns allow discriminating between patients and healthy controls, as well as among various types of dementia (e.g., Alzheimer dementia [AD] vs. frontotemporal dementia [FTD] (*4,5*)) and various types of parkinsonism (e.g., Parkinson disease vs. atypical parkinsonian syndromes (*3*)).

The parameters of ^{18}F-FDG PET examinations have to be chosen in a way that allows reliable identification of these patterns. Aside from technical factors such as scanner equipment and reconstruction, the image quality and noise level of ^{18}F-FDG PET scans are governed by 2 main parameters: administered activity and acquisition time.

Current state-of-the-art scan protocols involve an administered activity of about 200 MBq of ^{18}F-FDG and an acquisition time of 10 min. For example, the European Association of Nuclear Medicine procedure guidelines (*6*) propose 125–250 MBq and an acquisition of 15–30 min with a minimum of 10–15 min. Practice guidelines by the American College of Radiology imply 185–444 MBq and at least 10 min for the emission scan (*7*). The Society of Nuclear Medicine and Molecular Imaging recommends an administered activity of 185–740 MBq, with the upper limit being used for a 5-min emission scan (*8*). Radiation protection principles imply a radiation exposure as low as reasonably achievable and thus an ongoing effort to find possibilities for dose reduction. This is particularly true for pediatric patients and research studies with healthy controls. Moreover, a short acquisition is desirable in terms of patient comfort and compliance.

In the present study, we evaluated the potential for reducing acquisition time and administered activity. Both quantitative statistical analyses and visual reads were used to determine a minimum level of activity or acquisition time without compromised diagnostic outcome in patients with AD or FTD.

MATERIALS AND METHODS

Patients

This retrospective study included a sample of 13 patients with AD and 12 patients with FTD who were examined with ^{18}F-FDG PET as part of the routine diagnostics. Diagnoses were established by an interdisciplinary consensus panel based on comprehensive clinical and imaging work-up including ^{11}C-Pittsburgh compound B PET. Mean age was 67 ± 8 y for AD patients and 68 ± 7 for FTD patients. Mean mini-mental state examination score was 20.3 ± 4.4 for AD

Received Feb. 6, 2019; revision accepted Apr. 16, 2019.
For correspondence or reprints contact: Florian Schiller, Department of Nuclear Medicine, Medical Center–University of Freiburg, Hugstetter Strasse 55, 79106 Freiburg, Germany.
E-mail: florian.schiller@uniklinik-freiburg.de
Published online Apr. 26, 2019.

patients and 23.0 ± 5.3 for FTD patients (available in 12/13 and 10/12 patients, respectively). Mean clinical follow-up after the ^{18}F-FDG scan was 1.2 ± 1.1 y. All patients gave written informed consent to a retrospective data analysis, as approved by the local ethics committee.

PET Acquisition and Reconstruction

PET data acquisition was started 50 min after injection of 210 ± 9 MBq of ^{18}F-FDG under resting conditions (eyes open, ears unplugged) using a Gemini TF 64 (Philips) 3-dimensional time-of-flight PET/CT scanner with pixelated (yttrium-doped) lutetium oxyorthosilicate also called lutetium yttrium oxyorthosilicate (LYSO) crystals, an axial field of view of 18 cm, and a count rate performance typical for a first-generation time-of-flight PET device (*9*). The list-mode data were reconstructed to images with $2 \times 2 \times 2$ mm voxel size using the vendor-specific line-of-response row-action maximum-likelihood algorithm with 3 iterations and 33 subsets. To simulate reduced acquisition times or administered activity, the list-mode data of the PET examinations were reconstructed with various reduced acquisition times of 2, 6, 10, 20, and 30 s and 1 to 10 min in 1-min steps, centered on 55 min after injection.

Data Analysis

Volume-of-Interest (VOI)–Based Statistical Analyses. For statistical data analysis, spatial normalization was performed using the "Deform" brain normalization algorithm (without spatial filtering) as implemented in PMOD (version 3.7; PMOD Technologies) and the "PET HFS" ^{18}F-FDG brain template provided by the software. For each patient, the transformation matrix was derived with the 10-min reconstructions and applied to all other data sets to avoid bias from different coregistration results. Data sets were read out using VOIs from the automated anatomical labeling (AAL) template, as provided by PMOD. Each reconstructed image was then normalized to its cerebellar activity using all cerebellum VOIs defined by the template.

VOI-based analyses using these normalized uptakes were focused on a selection of brain regions that are of particular interest for the diagnosis of AD and FTD: the temporal, parietal, and frontal lobes and the precuneus and posterior cingulate cortex. Means and SDs were extracted and examined in terms of their dependence on reduced acquisition times. An independent *t* test was used to evaluate the significance of group differences between the AD and FTD groups at identical acquisition times.

Voxelwise Statistical Analyses. For each acquisition time, an image was calculated representing the voxelwise SD of each group. The dependence of the voxelwise SD on acquisition time was analyzed over the whole brain and over the aforementioned VOIs as an indicator for statistical noise.

Voxelwise group contrasts were evaluated with SPM12 (www.fil.ion.ucl.ac.uk/spm) using independent *t* tests with unequal variance after smoothing of each image with gaussian filtering (10 mm in full width at half maximum). Results were considered significant at a *P*-value of less than 0.001 at the voxel level with a cluster extent of more than 30 contiguous voxels.

Visual Reads. PET scans of all patients and selected acquisition times (10, 7, 5, 3, 2, 1, and 0.5 min) were visually rated by 3 independent, experienced readers using 30 transaxial slices covering the entire brain. In addition, readers had access to 3-dimensional stereotactic surface projections (3DSSP) depicting each individual's cerebral ^{18}F-FDG uptake and its statistical deviation from age-matched healthy controls (color-coded *z* score, 0–7; decreases only). 3DSSPs were created using the Neurostat 3DSSP software package from University of Washington (*10*) and a local database of healthy volunteers (both sexes) of a comparable age range.

Masking of all images with respect to patient identification and acquisition time, as well as mixing of all images, was performed to minimize bias. The readers were asked to provide a diagnosis including diagnostic certainty by returning integer numbers for which positive and negative values indicate AD and FTD, respectively. An absolute value of 3 indicates a definite diagnosis or clear-cut disease-specific pattern, a value of 2 indicates a probable diagnosis with moderate pattern expression or possibly only minor atypical features, a value of 1 indicates a possible diagnosis with only questionable or weak pattern expression or substantial atypical features, and a value of 0 indicates an indeterminate result.

RESULTS

PET Acquisition and Image Statistics

The administered activity resulted in total counts (prompt coincidences) within the entire field of view of $1.6 \pm 0.4 \times 10^8$ (range, $0.8–2.4 \times 10^8$) at 10 min to $3.1 \pm 0.7 \times 10^7$ (range, $1.7–4.7 \times 10^7$) at 2 min and $7.8 \pm 1.9 \times 10^6$ (range, $4.2–11.8 \times 10^6$) at 30 s. The counts decrease approximately in a linear fashion with reduced acquisition times. The average brain volume of the 25 patients was 1,311 ± 140 cm^3, with an average activity concentration of 13.3 ± 3.9 kBq/cm^3.

VOI-Based Statistical Analyses

Figure 1 illustrates normalized mean regional ^{18}F-FDG uptake in the selected regions as a function of reduced acquisition time. Mean values and SDs remain stable down to an acquisition time of 1 min in all considered regions. Except for the uptake in the posterior cingulate cortex of a few patients, no value deviates more than 5% from the original one at 10 min down to an acquisition time of 30 s.

To study a minimum acquisition time below which a distinction between the AD and FTD groups is severely hampered, *t* tests between the 2 groups were performed. Figure 2 shows the results as a function of reduced acquisition time for the selected brain regions. Mean ^{18}F-FDG uptake shows significant differences between the 2 groups down to 6 s, 10 s, and 30 s in the precuneus, parietal lobe, and posterior cingulate cortex, respectively. The *P*-value for the temporal lobe starts slightly above 0.05 and closely fluctuates arounds this value until 30 s. The group differences of the frontal region were not significant.

Voxelwise Statistical Analyses

With respect to the original 10-min acquisition time, the voxelwise SD among the patients of the AD and FTD groups increases at first moderately by 11% and 10%, respectively, at 2 min; then at 23% and 19%, respectively, at 1 min; and finally at 233% and 239%, respectively, at 2 s, as determined over the whole brain. This general behavior is also visible for region-based considerations as shown in Figure 3 for the 5 diagnostically important brain regions. Here, the increase is even lower, at 19% and 16%, respectively, at 1 min. Below a 1-min acquisition time, the deviations increase exponentially.

Results for the voxelwise group contrasts as determined with SPM12 ($P < 0.001$, $k \geq 30$ voxel) are shown in Figure 4. The pattern of significantly different clusters is stable when the acquisition time is reduced from 10 to 2 min, as the number of voxels decreases only slightly, by 5%, compared with the number of voxels at 10 min. At 1 min, some clusters appear noticeably smaller and even new clusters appear. From 30 s on, there is a pronounced decrease in the number of voxels resulting in 4,925 (46%) at 10 s. This decrease is accompanied by a noisier pattern.

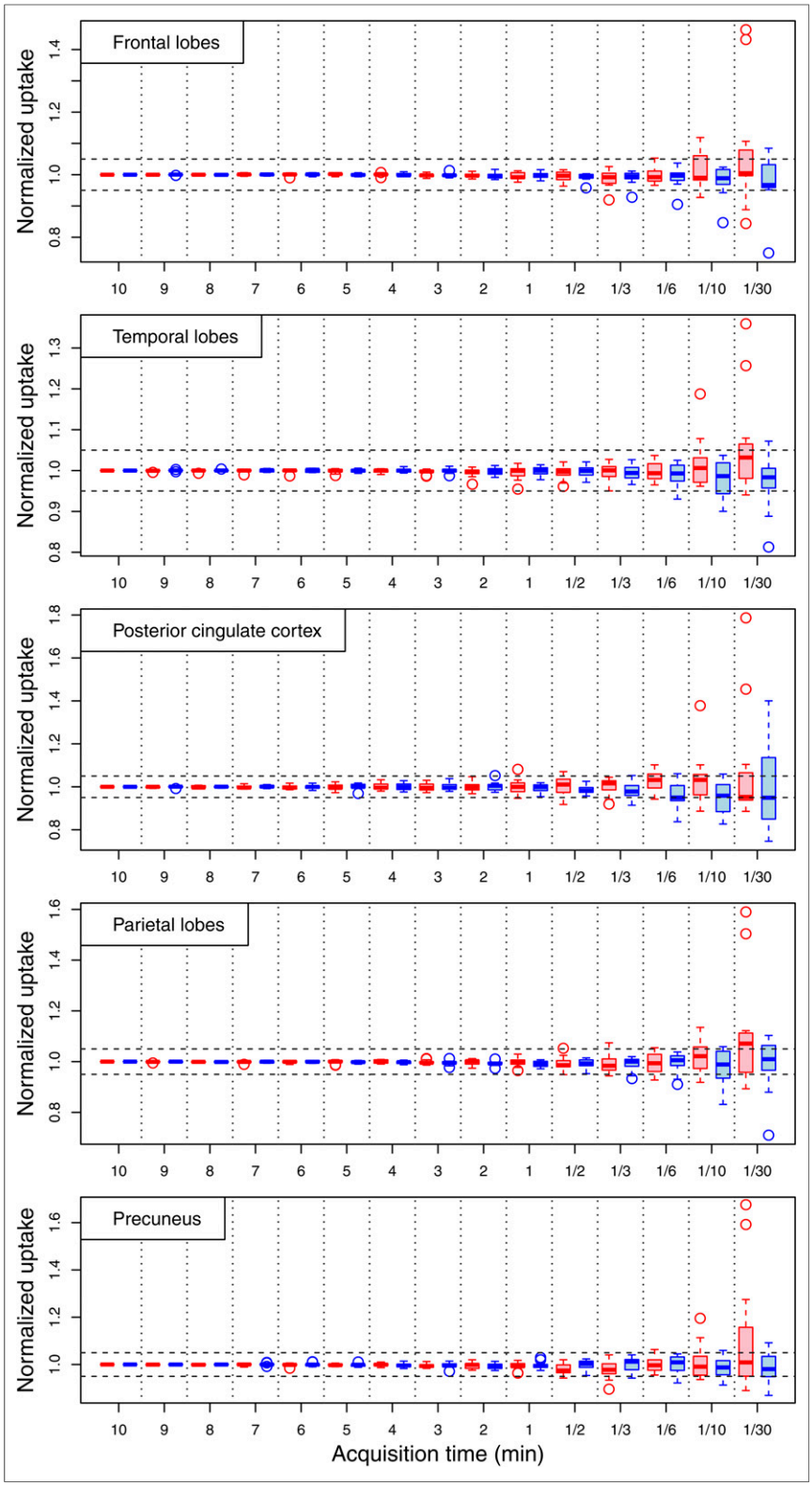

FIGURE 1. Box plots of regional mean uptake in all patients as function of acquisition time. Values were normalized to individual uptake in corresponding region at 10 min. Red and blue symbols indicate AD and FTD groups, respectively. Horizontal dashed lines mark deviation of 5% from original value. Whiskers are calculated from data according to Tukey method from interquartile distance (*26*), whereas outliers are indicated by circles.

Visual Reads

Three independent readers performed visual interpretations of images with 7 different acquisition times (10, 7, 5, 3, 2, 1, and 0.5 min) for each of the 25 patients of both groups (i.e., 175 scans in total). Examples of the primary image quality for an AD patient and an FTD patient (patients 4 and 25, respectively) are shown in Supplemental Figure 1 (supplemental materials are available at http://jnm.snmjournals.org). Visual readings were supported by *z* score maps provided by Neurostat/3DSSP as illustrated in Figure 5 for the same patients at various acquisition times. Both patients exhibited a moderately certain diagnosis (±1 or ±2) at the longer acquisition times, according to the 3 readers.

The results from the 3 readers are presented in Figure 6. There is agreement between this ^{18}F-FDG PET diagnosis and the consensus diagnosis including ^{11}C-Pittsburgh compound B PET and clinical follow-up in all but 3 patients (patients 8, 22, and 24). In 1 additional patient (patient 3), 2 of 3 readers found FTD instead of AD at a very low confidence level.

Figure 6 shows a stable pattern for all readers down to an acquisition time of around 2 min. Changes in diagnostic certainty from one acquisition time to the next shorter one are never larger than 1 except for reader 3 and patient 18 (from −3 to −1); however, this change is already reduced in the next shorter time. Most diagnostic certainties do not start to decrease until the step from 3 to 2 min or even 2 to 1 min.

Combining all 3 readers, 75 diagnoses based on acquisition times of 10 min were obtained. Using these as a reference, 450 rediagnoses were performed at reduced acquisition times. The first (absolute) change in diagnostic certainty by at least 2 with respect to the reference value at 10 min occurred for reader 1 at a 1-min acquisition time for 1 patient (patient 22) and 8 of 25 patients at 30 s. Reader 2 found the first change by 2 at 1 min for 1 patient (patient 7) and 5 of 25 patients at 30 s, whereas reader 3 reported 2 patients at each acquisition time of 3 min or shorter.

None of the 450 rediagnoses yielded a diagnosis change from AD to FTD or vice versa (i.e., a reversed sign). Moreover, a definite AD or FTD pattern (−3 or 3) at 10 min never turned into an indeterminate diagnosis even at the shortest acquisition time of 30 s.

For the rest of the analysis, we focused on diagnostic certainties, that is, the absolute

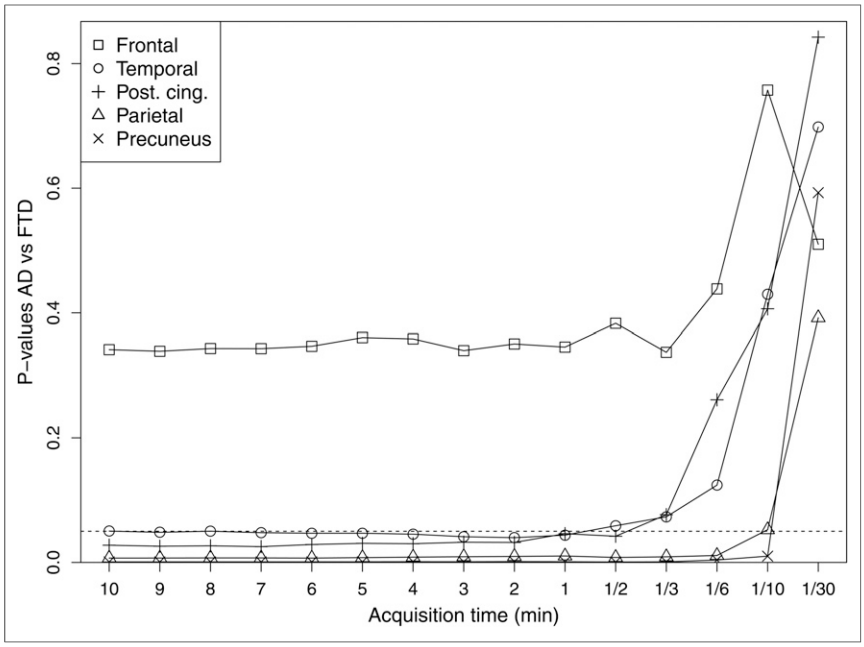

FIGURE 2. *P*-values from region-based independent *t* tests between AD and FTD groups for different acquisition times. Each symbol represents different region of brain as indicated. Dashed line indicates *P*-value of 0.05.

values of the diagnostic results. Corresponding means over all patients, SDs, and effect sizes (Cohen's d) are shown in Figure 7. Until an acquisition time of 2 min, only marginal decreases in certainty can be observed.

The effect size (Cohen's d) as presented in Figure 7 compared the distribution of diagnostic certainties at each acquisition time with respect to the situation at 10 min. Cohen's d was still around 0.3 at 2 min, implying a small effect according to Sawilowsky (*11*) whereas increasing to approximately 1 (large effect) at 1 min and below.

In addition, we tested the effect size of the difference in diagnostic results between the AD and FTD groups. The effect size ranged from 1.6 to 1.8 at 10 min throughout the 3 readers, that is, very large to huge effects (*11*). This effect size remained extremely stable, slightly dropping to 1.4–1.6 at 30 s but still representing very large to huge effects.

DISCUSSION

The current study provides a systematic analysis of the effect of acquisition time or, equivalently, administered activity on ^{18}F-FDG PET in dementia (AD vs. FTD, in particular). State-of-the-art guidelines for ^{18}F-FDG PET brain imaging typically recommend an administered activity of around 200 MBq (i.e., slightly below 3 MBq/kg of body weight in a typical 70-kg patient) and an acquisition time of at least 10 min (*6*–*8*).

The first step in our study—a VOI-based analysis—yields stable results down to an acquisition time of 1 min with few exceptions (in the small region of the posterior cingulate cortex). This finding holds true both for the mean values alone and for the group differences (Figs. 1 and 2).

In the more sophisticated, voxelwise, analysis that was the second step of our study, a more pronounced increase is seen around acquisition times of 2 min and below (Fig. 4). Moreover, the voxelwise group contrasts reveal a stable pattern until 2 min. Below this acquisition time, several clusters with significant differences start to shrink and new clusters may appear.

In the third and clinically most important step, we focused on single-subject diagnoses (AD vs. FTD) from visual readings at shorter acquisition times. Within 1 reader and 1 patient, changes of 1 in the diagnostic result may be due to an inherent uncertainty in visual reads and not necessarily the reduced image quality. In particular, there are many examples in which the result switches back and forth by 1. Because the first systematic and noticeable changes in diagnosis occur at 3 to 2 min, depending on the reader (Figs. 6 and 7), we conclude that this reduction by a factor of 4 is the limit for safe acquisition-time reductions.

Current studies on the requirements for dose or acquisition time in brain ^{18}F-FDG studies are rare. In a study by Chen et al. (*12*) from 2005 using a 2-dimensional PET acquisition on a scanner with bismuth germanate crystals and a 511-keV transmission scan for attenuation correction, the acquisition

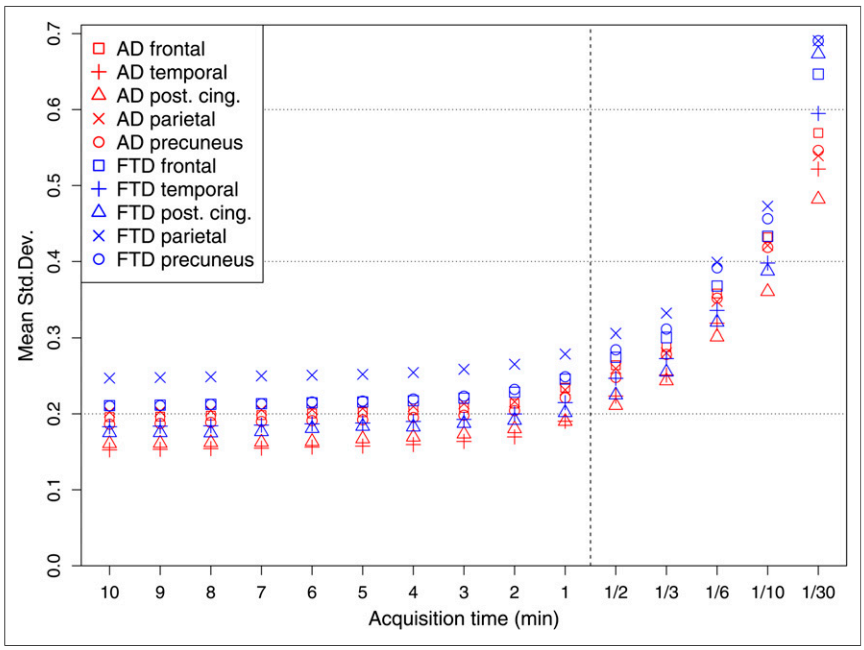

FIGURE 3. Voxelwise SD of regional ^{18}F-FDG uptake normalized to cerebellar uptake for subjects within AD and FTD groups. Shown are average values of SD within diagnostically relevant brain regions/VOIs from AAL template: frontal, temporal, and parietal regions as well as precuneus and posterior cingulate cortex. *x*-axis is stretched for acquisition times below 1 min.

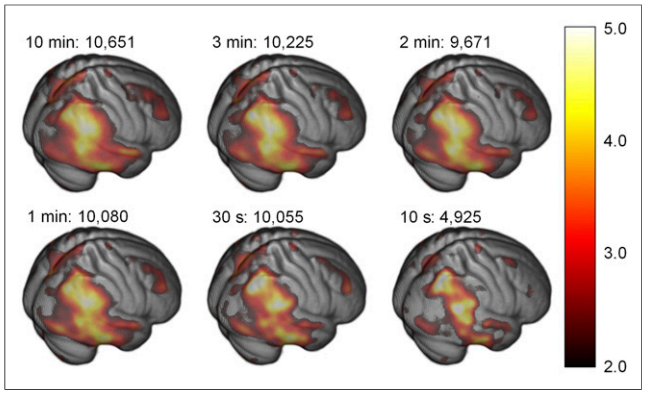

FIGURE 4. Map of T-values (in color) from voxelwise group contrasts as evaluated with SPM12 in independent *t* tests (hypothesis: FTD > AD). Selected acquisition times and numbers of voxels in statistically significant clusters are indicated. Clusters were regarded as significant if *P* was less than 0.001 at voxel level with cluster extent of more than 30 contiguous voxels.

time was reduced from 10 to 3 min while injecting about 400 MBq of ^{18}F-FDG. The mean values in various brain regions differed by 2.3% at most—comparable to the present study, which was performed with a lower administered activity and a 3-dimensional acquisition on a LYSO PET scanner with a higher count-rate performance (Fig. 1). Diagnostic performance was tested in receiver-operating-characteristic analyses using average uptake values in selected brain regions compared with the clinical diagnosis. In contrast to the present study, visual readings, which represent the clinical standard, were not performed. In addition, the protocol consisted of 2 different acquisitions separated by 20 min, which may have introduced systematic effects leading to the minor differences reported in this study.

A more recent study (n = 17), by Fällmar et al. (*13*), examined the effect of a reduction of administered activity by a factor of 4 (from 3 to 0.75 MBq/kg) on PET or PET/CT with bismuth germanate crystals in 3-dimensional acquisition mode but without time-of-flight capability. The low-dose ^{18}F-FDG PET was performed on average 26 d later in a separate scan. A small subgroup of patients (n = 5) was also examined with an even lower dose (one tenth, or 0.3 MBq/kg) on a different PET scanner using transmission attenuation correction. With respect to the factor 4 reductions, mean absolute differences were maximally 2.1% different from the original scans. For the factor 10 dose reductions, a 4.7% difference was found. This result agrees well with the present study (Fig. 3). The small region of the posterior cingulate cortex showing a larger variation here was treated separately in the present study, in contrast to the previous one (*13*). In a follow-up study (n = 9), a normal-dose PET scan and an additional low-dose PET scan with one fourth the administered activity were acquired on separate occasions and analyzed quantitatively and visually (*14*). Highly similar z scores from comparisons to healthy controls were found for both protocols.

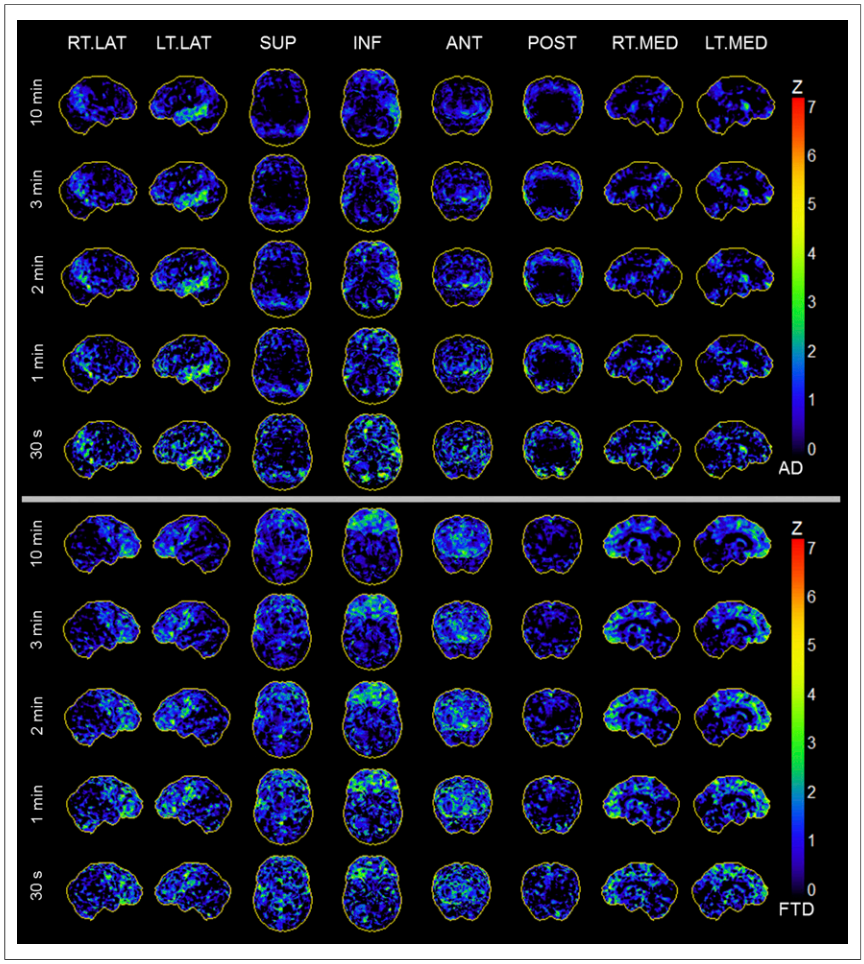

FIGURE 5. Results of Neurostat 3DSSP analysis as used for clinical evaluation of AD patient 4 and FTD patient 25: decrease in regional ^{18}F-FDG uptake normalized to cerebellum and color-coded as z score. Effect of reduced acquisition time is presented starting from standard duration of 10 min down to 30 s.

Zeimpekis et al. (*15*) also found stable uptake at simulated acquisition times of 3 min instead of 10 min (3 MBq/kg) but a pronounced decrease in image quality by 44%, which is at variance with the present study. However, the effect on diagnostic outcome was not studied in their sample of 5 patients. Kang et al. (*16*) tested algorithms for compensating quality losses of low-dose PET (~50 MBq instead of 200 MBq with 12-min acquisitions each) using PET/MRI in 11 patients and found deviations of 3% for the mean values in selected brain regions. This result supports the potential for significant reductions in acquisition time or administered activity, as we find in the current work even without advanced processing of the lower-quality scans.

In the present study, use of the original list-mode data for obtaining images at reduced acquisition times avoids possible systematic effects due to repeated scanning or even changing scanner hardware as in previous studies. The systematic coverage of 15 different acquisition times for each

Pat. ID	Diagn.	Results reader 1							Results reader 2							Results reader 3						
		Acquisition time (min)							Acquisition time (min)							Acquisition time (min)						
		10	7	5	3	2	1	0.5	10	7	5	3	2	1	0.5	10	7	5	3	2	1	0.5
1	AD	3	3	3	3	3	2	2	2	2	2	2	2	2	2	3	2	2	2	2	3	2
2	AD	1	1	1	1	1	0	0	1	1	0	1	1	0	0	1	0	1	0	0	0	0
3	AD	-1	-1	-1	-1	-1	0	0	2	1	1	2	2	1	1	-1	-1	-1	-1	0	-1	0
4	AD	1	2	2	2	1	1	1	1	1	1	1	1	2	1	1	1	1	1	1	1	1
5	AD	3	3	3	3	3	2	2	2	2	3	2	2	2	2	2	2	2	2	2	2	2
6	AD	3	3	3	3	3	2	2	3	3	3	3	2	2	2	3	3	3	3	3	2	3
7	AD	2	3	3	2	2	2	1	3	2	2	2	2	1	1	2	2	3	2	2	2	1
8	AD	-3	-3	-3	-3	-3	-3	-2	-3	-3	-3	-3	-3	-2	-2	-3	-3	-3	-3	-3	-3	-2
9	AD	2	2	2	2	2	1	1	1	1	1	1	2	1	0	1	2	1	1	1	1	1
10	AD	3	2	3	2	2	2	1	2	2	2	2	2	2	1	2	3	3	2	2	2	1
11	AD	3	3	3	3	3	2	2	2	3	2	2	3	2	1	3	3	3	3	3	3	2
12	AD	2	2	3	2	2	1	1	1	2	2	2	1	1	1	2	2	1	0	0	1	1
13	AD	2	2	2	1	2	1	1	2	2	2	2	1	1	0	2	2	2	1	2	2	1
14	FTD	-3	-2	-3	-3	-2	-2	-1	-2	-2	-2	-2	-2	-2	-1	-3	-3	-3	-3	-3	-2	-2
15	FTD	-2	-2	-2	-2	-2	-1	-1	-2	-2	-2	-2	-2	-2	-1	-2	-1	-2	-1	-2	-1	-1
16	FTD	-2	-2	-2	-1	-1	-1	0	-1	-1	-1	-1	-1	0	0	-1	-1	-1	-1	-1	-1	-1
17	FTD	-3	-3	-3	-3	-3	-2	-2	-3	-2	-3	-3	-2	-2	-2	-3	-3	-3	-3	-3	-3	-3
18	FTD	-3	-3	-3	-3	-2	-2	-1	-2	-3	-2	-2	-2	-1	0	-3	-2	-3	-1	-2	-1	-1
19	FTD	-3	-3	-3	-3	-3	-2	-2	-3	-3	-3	-3	-2	-2	-2	-3	-3	-3	-2	-2	-2	-2
20	FTD	-3	-3	-3	-2	-3	-2	-1	-2	-2	-3	-2	-2	-1	-1	-3	-3	-3	-3	-2	-2	-2
21	FTD	-3	-3	-3	-3	-3	-3	-2	-3	-2	-3	-2	-2	-2	-2	-2	-1	-2	-3	-2	-2	-1
22	FTD	3	3	3	2	2	1	1	3	3	3	2	2	2	1	3	2	2	2	1	1	1
23	FTD	-3	-3	-3	-3	-3	-2	-1	-3	-3	-3	-3	-3	-2	-1	-3	-3	-3	-3	-3	-2	-2
24	FTD	2	2	2	2	2	2	2	2	2	2	2	2	2	1	2	2	2	2	2	2	2
25	FTD	-2	-2	-2	-2	-2	-1	0	-2	-1	-2	-1	-1	-1	-1	-2	-2	-2	-2	-2	-2	-1
Sum |ΔDX|		0	4	3	6	5	20	31	0	12	10	15	18	27	36	0	9	8	14	15	17	25

FIGURE 6. Summary of diagnostic results of 3 independent readers for all patients and acquisition times from ^{18}F-FDG PET. Values indicate diagnosis as well as certainty ranging from −3 (definite FTD pattern) to +3 (definite AD pattern). Colors highlight results, with red indicating diagnosis of AD and blue FTD. Saturation reflects readers' certainty. Last line shows sum of absolute changes in diagnostic certainty (i.e., improved as well as impaired) over all patients with respect to results at 10 min.

patient allowed accurately identifying a safe margin for reducing acquisition time or administered activity. A key aspect in this regard was the visual reads being performed in parallel on the same images as in the quantitative analyses.

A reduced administered activity may lead to better performance of the PET camera in terms of the fraction of true versus random coincidences and the dead time. Thus, the possible savings in acquisition time may be expected to equal that in administered activity, suggesting that a reduction to approximately 50 MBq of administered activity may not compromise the outcome.

The acquisition was done on a PET/CT scanner with a low count-rate performance in comparison to other lutetium oxyorthosilicate (LSO) or LYSO PET/CT scanners. For comparison with NEMA performance measurements, which expresses performance in terms of noise-equivalent count rate, the noise-equivalent count rate of these scanners at an activity concentration of 13 kBq/cm^3 is typically between 90 kcps (for the scanner used in this study) and 150 kcps, depending on the size of the axial field of view (*9,17,18*). The noise-equivalent count rate of the latest generation of silicon-photomultiplier–based LYSO PET/CT scanner (*19–21*) is slightly higher (110–230 kcps at 13 kBq/cm^3, also strongly depending on the size of the axial field of view). We therefore assume that our results should be applicable to other LSO or LYSO PET/CT scanners with state-of-the-art iterative image reconstruction.

According to Brix et al. (*22*), relying on the current International Commission on Radiological Protection publications 103, 106, and 110 (*23–25*), the effective radiation dose due to a current standard administered activity of 200 MBq of ^{18}F-FDG for brain PET can be calculated to be 3.4 mSv. A possible reduced administered activity of 50 MBq would lower this dose to only 0.9 mSv.

Although the current study focused on AD and FTD, the derived potential for reducing acquisition time or administered activity may also apply to other neurodegenerative disorders of similar effect

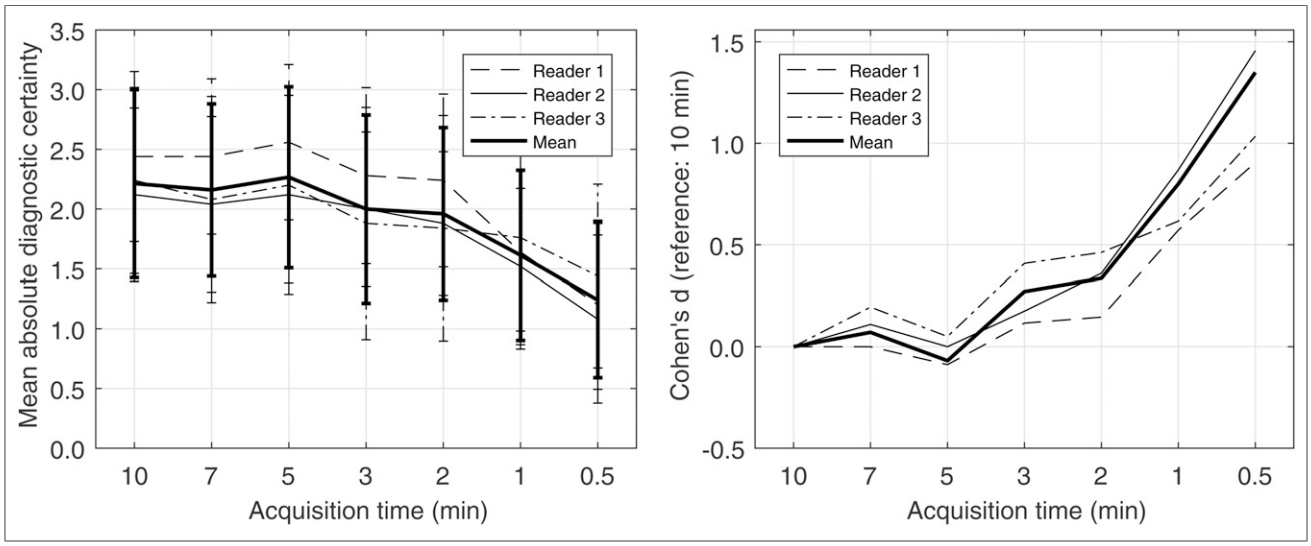

FIGURE 7. (Left) Mean absolute diagnostic certainty from visual reads, including SD, as function of acquisition time. (Right) Corresponding effect size (Cohen's d) compared with reference at 10 min. Results are presented separately for each reader and as mean over all 3 readers.

size. Beyond this application, dose reduction is of great importance, particularly for pediatric patients, follow-up examinations, and research studies on healthy controls, for which the present study may serve as a starting point for future systematic investigations.

CONCLUSION

Statistical results on a region level and a voxel level, as well as single-subject visual reads, reveal considerable potential to reduce the typical 10-min acquisition time (by a factor of 4) without compromising diagnostic quality. Conversely, our data suggest that for a given acquisition time of 10 min and a similar effect size, the administered activity may be reduced to 50 MBq, resulting in an effective dose of less than 1 mSv for the PET examination.

DISCLOSURE

No potential conflict of interest relevant to this article was reported.

KEY POINTS

QUESTION: What are the critical limits for reducing acquisition time and administered activity in brain ^{18}F-FDG PET studies in AD and FTD without compromising diagnostic quality?

PERTINENT FINDINGS: In a systematic, retrospective analysis of the ^{18}F-FDG PET data of 25 patients with AD or FTD, we demonstrated that reducing the acquisition time of 10 min (original data) by a factor of 4 did not relevantly affect region- and voxel-based statistical analyses or the visual reads of 3 independent raters. Conversely, our data suggest that for a given acquisition time of 10 min and a similar effect size, the administered activity may be reduced from about 200 MBq (original data) to only 50 MBq.

IMPLICATIONS FOR PATIENT CARE: Aside from potential advantages in terms of patient comfort and compliance (reduced acquisition time), the present study illustrates that it may be possible to reduce the effective dose of a brain ^{18}F-FDG PET examination from typically 3–4 mSv to less than 1 mSv.

REFERENCES

1. Bohnen NI, Djang DSW, Herholz K, Anzai Y, Minoshima S. Effectiveness and safety of ^{18}F-FDG PET in the evaluation of dementia: a review of the recent literature. *J Nucl Med.* 2012;53:59–71.
2. Herholz K. PET studies in dementia. *Ann Nucl Med.* 2003;17:79–89.
3. Meyer PT, Frings L, Rücker G, Hellwig S. ^{18}F-FDG PET in parkinsonism: differential diagnosis and evaluation of cognitive impairment. *J Nucl Med.* 2017; 58:1888–1898.
4. Mosconi L, Tsui WH, Herholz K, et al. Multicenter standardized ^{18}F-FDG PET diagnosis of mild cognitive impairment, Alzheimer's disease, and other dementias. *J Nucl Med.* 2008;49:390–398.
5. Foster NL, Heidebrink JL, Clark CM, et al. FDG-PET improves accuracy in distinguishing frontotemporal dementia and Alzheimer's disease. *Brain.* 2007;130: 2616–2635.
6. Varrone A, Asenbaum S, Vander Borght T, et al. EANM procedure guidelines for PET brain imaging using [^{18}F]FDG, version 2. *Eur J Nucl Med Mol Imaging.* 2009;36:2103–2110.
7. Frey KA, Lodge MA, Meltzer CC, et al. ACR-ASNR practice parameter for brain PET/CT imaging dementia. *Clin Nucl Med.* 2016;41:118–125.
8. Waxman AD, Herholz K, Lewis DH, et al. *Society of Nuclear Medicine Procedure Guideline for FDG PET Brain Imaging (Version 1.0).* Reston, VA: Society of Nuclear Medicine and Molecular Imaging; 2009.
9. Surti S, Kuhn A, Werner ME, Perkins AE, Kolthammer J, Karp JS. Performance of Philips Gemini TF PET/CT scanner with special consideration for its time-of-flight imaging capabilities. *J Nucl Med.* 2007;48:471–480.
10. Minoshima S, Frey KA, Koeppe RA, Foster NL, Kuhl DE. A diagnostic approach in Alzheimer's disease using three-dimensional stereotactic surface projections of fluorine-18-FDG PET. *J Nucl Med.* 1995;36:1238–1248.
11. Sawilowsky SS. New effect size rules of thumb. *J Mod Appl Stat Methods.* 2009;8:597–599.
12. Chen WP, Matsunari I, Noda A, et al. Rapid scanning protocol for brain ^{18}F-FDG PET: a validation study. *J Nucl Med.* 2005;46:1633–1641.
13. Fällmar D, Lilja J, Kilander L, et al. Validation of true low-dose ^{18}F-FDG PET of the brain. *Am J Nucl Med Mol Imaging.* 2016;6:269–276.
14. Fällmar D, Lilja J, Danfors T, et al. Z-score maps from low-dose ^{18}F-FDG PET of the brain in neurodegenerative dementia. *Am J Nucl Med Mol Imaging.* 2018;8: 239–246.
15. Zeimpekis KG, Barbosa F, Hüllner M, et al. Clinical evaluation of PET image quality as a function of acquisition time in a new TOF-PET/MRI compared to TOF-PET/CT: initial results. *Mol Imaging Biol.* 2015;17:735–744.
16. Kang J, Gao Y, Shi F, Lalush DS, Lin W, Shen D. Prediction of standard-dose brain PET image by using MRI and low-dose brain [^{18}F]FDG PET images. *Med Phys.* 2015;42:5301–5309.
17. Kemp BJ, Kim C, Williams JJ, Ganin A, Lowe VJ. NEMA NU 2-2001 performance measurements of an LYSO-based PET/CT system in 2D and 3D acquisition modes. *J Nucl Med.* 2006;47:1960–1967.
18. Rausch I, Cal-González J, Dapra D, et al. Performance evaluation of the Biograph mCT Flow PET/CT system according to the NEMA NU2-2012 standard. *EJNMMI Phys.* 2015;2:26.
19. Hsu DFC, Ilan E, Peterson WT, Uribe J, Lubberink M, Levin CS. Studies of a next-generation silicon-photomultiplier–based time-of-flight PET/CT system. *J Nucl Med.* 2017;58:1511–1518.
20. Rausch I, Ruiz A, Valverde-Pascual I, Cal-González J, Beyer T, Carrio I. Performance evaluation of the Vereos PET/CT system according to the NEMA NU2-2012 standard. *J Nucl Med.* 2019;60:561–567.
21. van Sluis JJ, de Jong J, Schaar J, et al. Performance characteristics of the digital Biograph Vision PET/CT system. *J Nucl Med.* 2019; 60:1031–1036.
22. Brix G, Nosske D, Lechel U. Radiation exposure of patients undergoing whole-body FDG-PET/CT examinations: an update pursuant to the new ICRP recommendations. *Nuklearmedizin.* 2014;53:217–220.
23. ICRP. The 2007 recommendations of the International Commission on Radiological Protection: ICRP publication 103. *Ann ICRP.* 2007;37:1–332.
24. ICRP. Radiation dose to patients from radiopharmaceuticals: addendum 3 to ICRP publication 53—ICRP publication 106. *Ann ICRP.* 2008;38:1–197.
25. ICRP. Adult reference computational phantoms: ICRP publication 110. *Ann ICRP.* 2009;39:1–164.
26. Beyer H. Tukey, John W.: Exploratory data analysis. Addison-Wesley Publishing Company Reading, Mass. – Menlo Park, Cal., London, Amsterdam, Don Mills, Ontario, Sydney 1977, XVI, 688 S [book review]. *Biometrical J.* 1981;23:413–414.